

## The Crystal Structure of 1,3,5-Triamino-2,4,6-trinitrobenzene\*

BY HOWARD H. CADY AND ALLEN C. LARSON

*University of California, Los Alamos Scientific Laboratory, Los Alamos, New Mexico, U.S.A.*

(Received 10 April 1964)

The crystal structure of 1,3,5-triamino-2,4,6-trinitrobenzene has been refined by full-matrix least-squares computations on all positional and thermal parameters, including hydrogen atoms, to a final  $R$  index of 0.053 for 928 reflections of observable intensity. The unit cell is triclinic,

$$P\bar{1}, a = 9.010, b = 9.028, c = 6.812 \text{ \AA}, \text{ and } \alpha = 108.59^\circ, \beta = 91.82^\circ, \gamma = 119.97^\circ,$$

with two molecules per cell. The refinement was made with both spherical and non-spherical atomic scattering factors for the carbon and oxygen atoms.

Three features of this structure are particularly unusual: the aromatic carbon-carbon distance of 1.444 Å, the carbon-amino nitrogen distance of 1.319 Å, and the presence of six bifurcated nitrogen-oxygen hydrogen bonds.

### Introduction

The compound 1,3,5-triamino-2,4,6-trinitrobenzene (TATB) is unusual in its thermal and solubility properties. The compound sublimes and decomposes above 300 °C. Concentrated sulfuric acid is the best of the few known solvents for TATB. These facts indicated that the compound would be of interest because of its hydrogen bonding system in which both inter- and intra-molecular hydrogen bonds are likely between amine groups and adjacent nitro groups.

Another compound, 1,3-diamino-2,4,6-trinitrobenzene, form I (Holden, 1962), that has a similar hydrogen bond system has been reported.

### Optical crystallography

Triclinic TATB crystals commonly exhibit the forms {001}, {100}, and {011}, and have nearly perfect cleavage parallel to {001}. The X optic axis is perpendicular to the  $a$ - $b$  plane, and the Y optic axis is 63.6° from  $b$  and 56.4° from  $a$ . The crystals are strongly pleochroic, being colorless parallel to the X axis and yellow in the Y-Z plane. The crystals are anisotropic and biaxial negative, with  $2E = 62.8^\circ$  and  $2V \approx 26^\circ$ , as estimated from a centered optic axis figure. The indices of refraction are  $n_x = 1.45$ , and estimating from  $2V$ ,  $n_y = 2.3$  and  $n_z = 3.1$ . Only one polymorph has been observed.

### Experimental

Single crystals suitable for optical and X-ray crystallography were obtained by recrystallization from hot nitrobenzene. A crystal having no dimension greater than 200  $\mu$  was selected for the determination of

the crystal structure. The crystal was aligned, and preliminary unit-cell dimensions were determined by using precession photographs. The crystal was then transferred to a carefully aligned General Electric Company Single Crystal Orienter (SCO) equipped with a scintillation counter and a molybdenum X-ray tube.

Cell dimensions were determined from a least-squares fit of 31  $2\theta$  ( $\lambda$  Mo  $K\alpha_1 = 0.70926$  Å) values, greater than 24°, for general  $hkl$  reflections which were measured on the SCO. This least-squares fit gives

$a = 9.010 \pm 0.003$ ,  $b = 9.028 \pm 0.003$ ,  $c = 6.812 \pm 0.003$  Å,  $\alpha = 108.59 \pm 0.02^\circ$ ,  $\beta = 91.82 \pm 0.03^\circ$ ,  $\gamma = 119.97 \pm 0.01^\circ$  for the triclinic unit-cell parameters. There are two molecules in the unit cell, and the calculated density of 1.937 g.cm<sup>-3</sup> compares favorably with the measured density of  $1.93 \pm 0.01$  g.cm<sup>-3</sup>. The crystal was mounted with its  $a^*$  axis coincident with the  $\varphi$  axis of the SCO. Background correction was made by the balanced filter technique. Reflections within a sphere limited by  $2\theta = 60^\circ$  were examined by the stationary counter, stationary crystal technique. No reflections were detected by film techniques at larger  $2\theta$  values. Within the hemisphere considered, 2597 reflections were examined, of which 928 were strong enough to be observed ( $I - B_{\text{kgd}} > 2.5\sqrt{I + B_{\text{kgd}}}$ ).

### Computational details

The usual Lorentz and polarization corrections were applied to give a set of observed  $|F_{hkl}|^2$  values on a relative scale. No absorption corrections were applied (abs. coeff. = 2.16 cm<sup>-1</sup>). In the later stages of the least-squares refinement, however, an extinction correction was included. Several different weighting schemes were applied.

All least-squares calculations were made by using the full matrix. One scale factor was used as a least-

\* Work performed under the auspices of the United States Atomic Energy Commission.

squares parameter, and in all cases where anisotropic temperature factors were used, a secondary extinction correction,  $g$ , was also included as a least-squares parameter. The observational equation was of the form

$$\Delta F = F_o - \frac{|F_c|}{k(1+gLp|F_c|^2)^{\frac{1}{2}}}$$

where

- $k$  = scale factor  
 $g$  = secondary extinction parameter  
 $Lp$  = Lorentz polarization factor.

Anisotropic thermal parameters were of the form

$$\exp \left\{ -(h^2 B_{11} + k^2 B_{22} + l^2 B_{33} + hk B_{12} + hl B_{13} + kl B_{23}) \right\}.$$

The function  $\sum w(|F_o| - |F_c|)^2$  was minimized. The  $R$  index ( $\sum ||F_o| - |F_c|| / \sum |F_o|$ ) was calculated ignoring unobserved reflections. The estimated standard deviations were calculated from

$$\sigma_j = \left( a^{jj} \left( \frac{\sum w(|F_o| - |F_c|)^2}{m-n} \right) \right)^{\frac{1}{2}}$$

where  $m$  is the number of observed reflections,  $n$  is the number of parameters, and  $a^{jj}$  is the  $jj$  element of the inverse matrix. Convergence acceleration methods were not used. The programs used in the calculations were written for the IBM 7094 computer by A. C. Larson, D. T. Cromer, R. B. Roof, or H. H. Cady of the Los Alamos Scientific Laboratory. A detailed description of these programs is to be published as a series of Los Alamos Scientific Laboratory reports. All Fourier maps were plotted using the General Dynamics Corporation S-C 4020 microfilm recorder.

### Determination and refinement of the structure

The space group is not uniquely determined by systematic extinctions and could be either  $P1$  or  $P\bar{1}$ . Statistical tests (Howells, 1950; Ramachandran, 1959) indicated that the proper space group was  $P\bar{1}$ . Because a satisfactory solution to the structure was found in  $P\bar{1}$ , it is assumed to be the correct space group.

Optical and cleavage properties of the crystal indicated that the molecules are arranged in planar sheets parallel to the  $a$ - $b$  plane. The strength of the 002 reflection, together with the absence of the 001, 003, 005, and 007 reflections, indicated that these planes are at  $z \approx \frac{1}{4}$  and  $\frac{3}{4}$ .

A three-dimensional sharpened Patterson function was computed which confirmed the choice for the planes of the molecules. The through-center vectors determined approximate  $x$  and  $y$  coordinates of all the non-hydrogen atoms.

The coordinates of the atoms in the molecule at  $z \approx \frac{1}{4}$  were used as starting parameters in a least-squares refinement. Form factors were used in functional form with parameters given by Forsyth & Wells (1959). All observed reflections were given unit weight, and isotropic temperature factors were applied. The problem quickly converged and showed that the trial structure was correct. After four cycles, the value of  $R$  was 0.17. All atoms were then allowed to become anisotropic, and an extinction correction was introduced as a variable and was adjusted in all following calculations. After three more cycles,  $R$  was reduced to 0.073. At this point, the 59 reflections for which  $||F_o| - |F_c|| \leq 2.0e$  were remeasured. With the corrected data,  $R$  dropped to 0.065. A difference Fourier synthesis was then calculated to locate hydrogen atoms. Peaks of about 0.4 e.Å<sup>-3</sup> in height were observed in reasonable locations. Peaks also could be seen on the observed Fourier syntheses in these positions.

Hydrogen atoms with isotropic thermal parameters were placed in these positions and their parameters included as variables for seven more cycles of least-squares refinement, and  $R$  dropped to 0.053. The positional parameters of the hydrogen atoms converged, but the thermal parameter of one of these atoms tended to become negative by one-fifth of its standard deviation. Three-dimensional observed and difference Fourier syntheses were calculated including contributions from all atoms. Only the sections in the vicinity of the molecule showed significant residual peaks of electron density in the difference Fourier synthesis. The sections through one molecule at  $z \approx \frac{1}{4}$  are shown in Figs. 1 and 2. It is apparent that the peaks of the difference Fourier synthesis are systematically located between the atoms. The standard deviation of the electron density ( $\sigma_e$ ) in the structure is estimated to be 0.07 e.Å<sup>-3</sup> by Cruickshank's (1949) formula. Although this is a somewhat low estimate because of the number of unobserved reflections, there are nine peaks in this section greater than  $3\sigma$ . This number of strong peaks and their systematic locations with respect to benzene ring and hydrogen bonds indicated that further refinement might be rewarding.

The possibility that the weighting scheme for the data caused these peaks in the difference Fourier

Table 1. Atomic scattering factors

Atom	Type	A	B	C	D	E
Carbon	$f^{\parallel}$	1.675	1.074	3.760	16.94	0.5465
Carbon	$f^{\perp}$	1.570	0.4682	4.297	21.21	0.1166
Oxygen	$f^{\parallel}$	1.023	0.3545	6.425	11.47	0.1166
Oxygen	$f^{\perp}$	1.419	1.233	5.609	10.54	0.9719

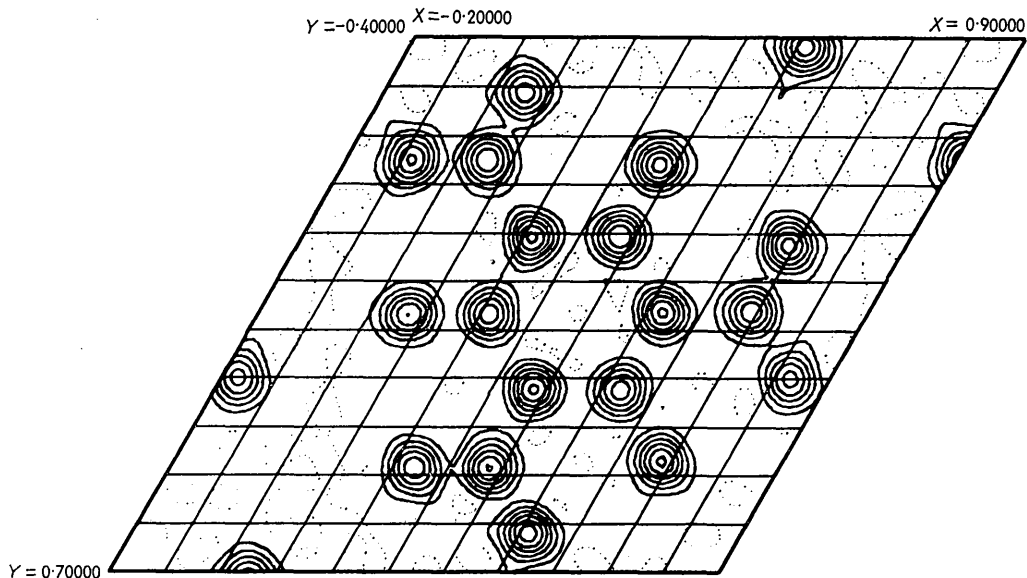


Fig. 1. The electron density in the section  $z = \frac{1}{4}$ . Contours are at intervals of  $2 \text{ e.}\text{\AA}^{-3}$ ; the zero contour is dotted.

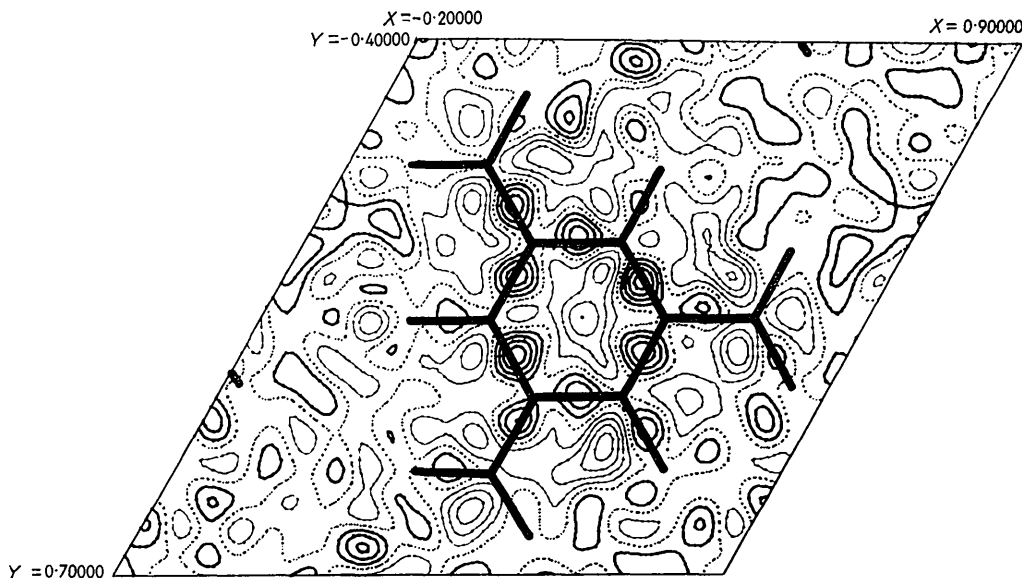


Fig. 2. The section  $z = \frac{1}{4}$  of a three-dimensional difference map. All atoms were included in the  $F(\text{calc.})$ 's, the heavy atoms having anisotropic temperature factors but spherical form factors. Contours are at intervals of  $0.067 \text{ e.}\text{\AA}^{-3}$ . The zero contour is dotted; negative contours are light, continuous lines.

synthesis was considered. Changing the weighting scheme in the least-squares calculations, however, had only a slight effect on either the difference Fourier synthesis or the results of the least-squares calculations. One of the two additional weighting schemes used in the least-squares calculations was to weight the data as  $1/\hat{f}$  ( $\hat{f} = (1/n)\sum f_n/Z_n$  for all atoms except hydrogen), which should give the same result as a Fourier analysis (Lipson & Cochran, 1957). The other scheme was to weight the data by the method of Evans (1961), which weights according to counting statistics.

At this point in the refinement, non-spherical atomic scattering factors were introduced into the least-squares calculation as a first approximation to bonding. The method of McWeeny (1951) was used. His values of  $f''$  and  $f'$  for carbon and oxygen atoms were transformed into the functional form of Forsyth & Wells (1959) by least-squares. This equation has the form  $f_{(s)} = A \exp(-Bs^2) + C \exp(-Ds^2) + E$ , where  $s = \sin \theta/\lambda$ . The values found for the constants in the equation are given in Table 1.

To simplify the coding problem, the TATB molecule was assumed to be planar, parallel to the  $a$ - $b$  plane,

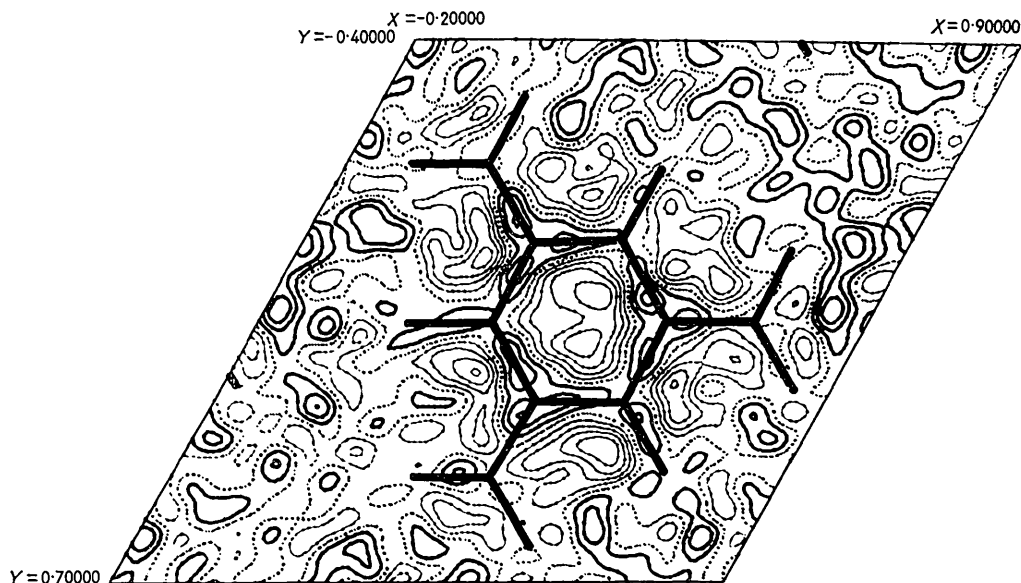


Fig. 3. The section  $z = \frac{1}{4}$  of a three-dimensional difference map, identical with that shown in Fig. 2 except that the  $F(\text{calc.})$ 's are based on non-spherical form factors for the carbon and oxygen atoms (see text).

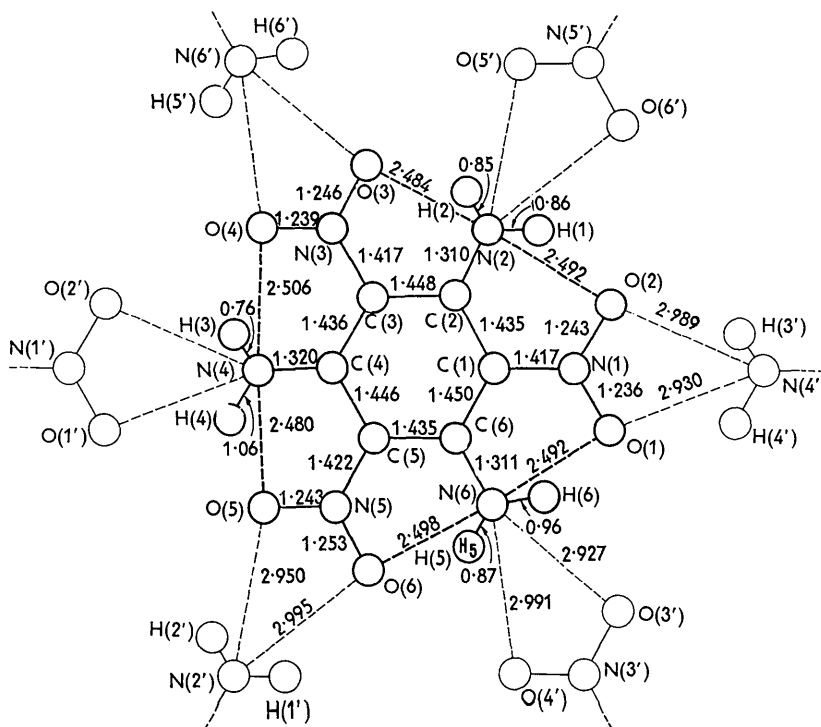


Fig. 4. Bond distances and hydrogen bonding in TATB.

and to have bond angles of  $120^\circ$ . It follows, then, that the unique direction for the carbon atoms would be perpendicular to the plane of the molecule, while the unique direction of the oxygen atoms would be in the plane of the molecule and perpendicular to the nitrogen-oxygen bonds. The data again were given unit weight for observed reflections in the least-

squares calculations. The problem quickly converged, giving an  $R$  index of 0.056. This slight increase in the  $R$  index was disappointing. On the other hand, the difference Fourier in the vicinity of the molecule showed some improvement. The section through the molecule which may be compared with Figs. 1 and 2 is shown in Fig. 3.

Table 2. Final TATB least-squares parameters, spherical  $f$ ,  $w=1.0$

Atom	$x$	$y$	$z$	$B_{11} \times 10^4$	$B_{22} \times 10^4$	$B_{33} \times 10^4$	$B_{12} \times 10^4$	$B_{13} \times 10^4$	$B_{23} \times 10^4$	$B$
C(1)	0.5334 ± 6	0.1657 ± 7	0.2569 ± 10	48 ± 8	76 ± 9	185 ± 20	59 ± 15	37 ± 22	124 ± 23	0.0 ± 11
C(2)	0.3733 ± 7	0.0027 ± 7	0.2485 ± 9	55 ± 8	77 ± 9	127 ± 18	73 ± 14	31 ± 19	69 ± 21	0.8 ± 13
C(3)	0.2155 ± 6	0.0072 ± 7	0.2486 ± 10	63 ± 9	62 ± 9	159 ± 18	51 ± 14	46 ± 20	93 ± 22	1.1 ± 14
C(4)	0.2147 ± 6	0.1666 ± 7	0.2511 ± 9	66 ± 8	73 ± 9	180 ± 19	83 ± 15	86 ± 21	116 ± 22	3.5 ± 19
C(5)	0.3754 ± 7	0.3219 ± 7	0.2444 ± 11	66 ± 9	84 ± 10	235 ± 21	94 ± 17	88 ± 24	181 ± 25	1.7 ± 15
C(6)	0.5380 ± 6	0.3269 ± 7	0.2522 ± 9	69 ± 8	77 ± 9	158 ± 18	72 ± 14	54 ± 20	97 ± 21	5.5 ± 23
N(1)	0.6926 ± 5	0.1686 ± 6	0.2702 ± 8	69 ± 8	90 ± 8	270 ± 18	86 ± 14	108 ± 20	191 ± 21	
N(2)	0.3689 ± 7	-0.1468 ± 7	0.2388 ± 10	78 ± 8	84 ± 9	336 ± 21	116 ± 14	160 ± 20	223 ± 22	
N(3)	0.0565 ± 5	-0.1494 ± 6	0.2467 ± 9	51 ± 7	94 ± 9	292 ± 19	58 ± 13	91 ± 19	206 ± 22	
N(4)	0.0712 ± 7	0.1725 ± 7	0.2580 ± 10	64 ± 7	98 ± 9	309 ± 21	100 ± 14	108 ± 20	180 ± 23	
N(5)	0.3741 ± 6	0.4761 ± 6	0.2344 ± 8	82 ± 7	93 ± 9	221 ± 17	103 ± 14	86 ± 18	167 ± 20	
N(6)	0.6849 ± 6	0.4709 ± 6	0.2516 ± 9	76 ± 8	74 ± 9	299 ± 20	60 ± 14	132 ± 21	198 ± 23	
O(1)	0.8354 ± 5	0.3070 ± 6	0.2824 ± 9	67 ± 7	137 ± 9	641 ± 25	117 ± 13	198 ± 21	401 ± 26	
O(2)	0.6930 ± 5	0.0298 ± 6	0.2645 ± 8	85 ± 7	136 ± 9	429 ± 19	158 ± 13	150 ± 19	284 ± 22	
O(3)	0.0510 ± 6	-0.2923 ± 6	0.2373 ± 10	99 ± 8	133 ± 9	690 ± 26	126 ± 14	223 ± 23	430 ± 27	
O(4)	-0.0812 ± 5	-0.1498 ± 6	0.2525 ± 9	62 ± 6	133 ± 8	483 ± 20	105 ± 12	200 ± 18	324 ± 22	
O(5)	0.2381 ± 5	0.4789 ± 6	0.2304 ± 9	108 ± 8	143 ± 9	515 ± 22	181 ± 15	155 ± 21	333 ± 24	
O(6)	0.5128 ± 5	0.6173 ± 5	0.2385 ± 8	88 ± 6	99 ± 8	412 ± 19	111 ± 12	134 ± 18	280 ± 20	
H(1)	0.4671 ± 76	-0.1426 ± 73	0.2354 ± 87							0.0 ± 11
H(2)	0.2722 ± 80	-0.2385 ± 83	0.2536 ± 96							0.8 ± 13
H(3)	-0.0214 ± 85	0.0854 ± 88	0.2517 ± 100							1.1 ± 14
H(4)	0.0708 ± 97	0.2881 ± 108	0.2559 ± 121							3.5 ± 19
H(5)	0.6801 ± 85	0.5664 ± 93	0.2473 ± 106							1.7 ± 15
H(6)	0.7957 ± 121	0.4592 ± 121	0.2311 ± 137							5.5 ± 23

Scale 2.548 ± 10 Extinction × 10<sup>7</sup> 8.32 ± 40

Table 3. Final TATB least-squares parameters, non-spherical  $f$ ,  $w=1.0$

Atom	$x$	$y$	$z$	$B_{11} \times 10^4$	$B_{22} \times 10^4$	$B_{33} \times 10^4$	$B_{12} \times 10^4$	$B_{13} \times 10^4$	$B_{23} \times 10^4$	$B$
C(1)	0.5332 ± 7	0.1651 ± 8	0.2568 ± 10	30 ± 9	55 ± 10	206 ± 21	44 ± 16	48 ± 23	141 ± 24	0.8 ± 15
C(2)	0.3733 ± 7	0.0026 ± 7	0.2487 ± 9	37 ± 8	60 ± 10	158 ± 19	60 ± 15	42 ± 21	83 ± 23	0.7 ± 14
C(3)	0.2150 ± 7	0.0073 ± 7	0.2487 ± 11	45 ± 9	45 ± 10	196 ± 20	49 ± 15	60 ± 22	117 ± 24	1.5 ± 18
C(4)	0.2144 ± 7	0.1667 ± 7	0.2511 ± 10	45 ± 9	55 ± 10	217 ± 20	62 ± 16	103 ± 22	141 ± 24	3.9 ± 22
C(5)	0.3760 ± 7	0.3218 ± 8	0.2442 ± 11	36 ± 9	61 ± 11	268 ± 22	64 ± 17	106 ± 25	192 ± 26	2.4 ± 18
C(6)	0.5379 ± 7	0.3268 ± 7	0.2520 ± 10	38 ± 9	60 ± 10	190 ± 19	57 ± 16	61 ± 22	124 ± 23	4.1 ± 23
N(1)	0.6921 ± 6	0.1683 ± 6	0.2695 ± 9	60 ± 8	83 ± 9	247 ± 19	83 ± 14	104 ± 21	176 ± 22	
N(2)	0.3693 ± 7	-0.1466 ± 7	0.2389 ± 11	81 ± 9	72 ± 8	308 ± 22	105 ± 15	151 ± 22	207 ± 23	
N(3)	0.0565 ± 6	-0.1493 ± 6	0.2467 ± 9	48 ± 8	87 ± 9	267 ± 19	58 ± 13	85 ± 20	188 ± 23	
N(4)	0.0710 ± 7	0.1722 ± 7	0.2578 ± 11	54 ± 8	99 ± 10	292 ± 22	97 ± 15	96 ± 21	174 ± 24	
N(5)	0.3747 ± 6	0.4763 ± 6	0.2350 ± 8	70 ± 8	82 ± 9	205 ± 18	96 ± 14	83 ± 19	151 ± 21	
N(6)	0.6842 ± 6	0.4709 ± 7	0.2517 ± 10	64 ± 9	67 ± 9	288 ± 22	49 ± 15	127 ± 23	185 ± 24	
O(1)	0.8335 ± 5	0.3069 ± 6	0.2820 ± 10	65 ± 7	141 ± 10	602 ± 27	108 ± 14	176 ± 23	370 ± 28	
O(2)	0.6927 ± 6	0.0297 ± 6	0.2641 ± 9	95 ± 7	142 ± 10	373 ± 20	170 ± 14	141 ± 21	258 ± 24	
O(3)	0.0512 ± 6	-0.2919 ± 6	0.2377 ± 10	114 ± 9	130 ± 10	655 ± 28	133 ± 16	235 ± 25	416 ± 29	
O(4)	-0.0811 ± 5	-0.1499 ± 6	0.2525 ± 9	65 ± 7	150 ± 9	435 ± 22	110 ± 13	198 ± 20	326 ± 24	
O(5)	0.2380 ± 6	0.4789 ± 6	0.2304 ± 9	116 ± 9	153 ± 10	471 ± 24	194 ± 16	147 ± 23	338 ± 26	
O(6)	0.5131 ± 5	0.6175 ± 6	0.2387 ± 8	96 ± 7	98 ± 8	350 ± 20	98 ± 13	102 ± 20	249 ± 22	
H(1)	0.467 ± 9	-0.143 ± 9	0.238 ± 11							0.8 ± 15
H(2)	0.280 ± 9	-0.232 ± 9	0.260 ± 11							0.7 ± 14
H(3)	-0.017 ± 10	0.091 ± 10	0.254 ± 12							1.5 ± 18
H(4)	0.071 ± 11	0.288 ± 12	0.254 ± 14							3.9 ± 22
H(5)	0.682 ± 10	0.564 ± 11	0.244 ± 12							2.4 ± 18
H(6)	0.779 ± 11	0.454 ± 12	0.224 ± 14							4.1 ± 23

Scale 2.607 ± 11 Extinction × 10<sup>7</sup> 8.41 ± 40

Table 4. Observed and calculated magnitudes of the structure factors for *TATB*The column headings are  $l$ ,  $|10kF_o/[1-gLp(kF_o)^2]|$  and  $10F_c$ . A minus sign preceding  $F_o$  should be read as 'less than'

$h$	$0$	$k$	$l$	$10kF_o/[1-gLp(kF_o)^2]$	$10F_c$	$h$	$0$	$k$	$l$	$10kF_o/[1-gLp(kF_o)^2]$	$10F_c$	$h$	$0$	$k$	$l$	$10kF_o/[1-gLp(kF_o)^2]$	$10F_c$	$h$	$0$	$k$	$l$	$10kF_o/[1-gLp(kF_o)^2]$	$10F_c$	
1	0	0	0	1	1	1	0	0	0	1	1	1	0	0	0	1	1	1	0	0	0	1	1	1
2	0	0	0	4	4	2	0	0	0	4	4	2	0	0	0	4	4	2	0	0	0	4	4	2
3	0	0	0	9	9	3	0	0	0	9	9	3	0	0	0	9	9	3	0	0	0	9	9	3
4	0	0	0	16	16	4	0	0	0	16	16	4	0	0	0	16	16	4	0	0	0	16	16	4
5	0	0	0	25	25	5	0	0	0	25	25	5	0	0	0	25	25	5	0	0	0	25	25	5
6	0	0	0	36	36	6	0	0	0	36	36	6	0	0	0	36	36	6	0	0	0	36	36	6
7	0	0	0	49	49	7	0	0	0	49	49	7	0	0	0	49	49	7	0	0	0	49	49	7
8	0	0	0	64	64	8	0	0	0	64	64	8	0	0	0	64	64	8	0	0	0	64	64	8
9	0	0	0	81	81	9	0	0	0	81	81	9	0	0	0	81	81	9	0	0	0	81	81	9
10	0	0	0	100	100	10	0	0	0	100	100	10	0	0	0	100	100	10	0	0	0	100	100	10
11	0	0	0	121	121	11	0	0	0	121	121	11	0	0	0	121	121	11	0	0	0	121	121	11
12	0	0	0	144	144	12	0	0	0	144	144	12	0	0	0	144	144	12	0	0	0	144	144	12
13	0	0	0	169	169	13	0	0	0	169	169	13	0	0	0	169	169	13	0	0	0	169	169	13
14	0	0	0	196	196	14	0	0	0	196	196	14	0	0	0	196	196	14	0	0	0	196	196	14
15	0	0	0	225	225	15	0	0	0	225	225	15	0	0	0	225	225	15	0	0	0	225	225	15
16	0	0	0	256	256	16	0	0	0	256	256	16	0	0	0	256	256	16	0	0	0	256	256	16
17	0	0	0	289	289	17	0	0	0	289	289	17	0	0	0	289	289	17	0	0	0	289	289	17
18	0	0	0	324	324	18	0	0	0	324	324	18	0	0	0	324	324	18	0	0	0	324	324	18
19	0	0	0	361	361	19	0	0	0	361	361	19	0	0	0	361	361	19	0	0	0	361	361	19
20	0	0	0	400	400	20	0	0	0	400	400	20	0	0	0	400	400	20	0	0	0	400	400	20
21	0	0	0	441	441	21	0	0	0	441	441	21	0	0	0	441	441	21	0	0	0	441	441	21
22	0	0	0	484	484	22	0	0	0	484	484	22	0	0	0	484	484	22	0	0	0	484	484	22
23	0	0	0	529	529	23	0	0	0	529	529	23	0	0	0	529	529	23	0	0	0	529	529	23
24	0	0	0	576	576	24	0	0	0	576	576	24	0	0	0	576	576	24	0	0	0	576	576	24
25	0	0	0	625	625	25	0	0	0	625	625	25	0	0	0	625	625	25	0	0	0	625	625	25
26	0	0	0	676	676	26	0	0	0	676	676	26	0	0	0	676	676	26	0	0	0	676	676	26
27	0	0	0	729	729	27	0	0	0	729	729	27	0	0	0	729	729	27	0	0	0	729	729	27
28	0	0	0	784	784	28	0	0	0	784	784	28	0	0	0	784	784	28	0	0	0	784	784	28
29	0	0	0	841	841	29	0	0	0	841	841	29	0	0	0	841	841	29	0	0	0	841	841	29
30	0	0	0	900	900	30	0	0	0	900	900	30	0	0	0	900	900	30	0	0	0	900	900	30
31	0	0	0	961	961	31	0	0	0	961	961	31	0	0	0	961	961	31	0	0	0	961	961	31
32	0	0	0	1024	1024	32	0	0	0	1024	1024	32	0	0	0	1024	1024	32	0	0	0	1024	1024	32
33	0	0	0	1089	1089	33	0	0	0	1089	1089	33	0	0	0	1089	1089	33	0	0	0	1089	1089	33
34	0	0	0	1156	1156	34	0	0	0	1156	1156	34	0	0	0	1156	1156	34	0	0	0	1156	1156	34
35	0	0	0	1225	1225	35	0	0	0	1225	1225	35	0	0	0	1225	1225	35	0	0	0	1225	1225	35
36	0	0	0	1296	1296	36	0	0	0	1296	1296	36	0	0	0	1296	1296	36	0	0	0	1296	1296	36
37	0	0	0	1369	1369	37	0	0	0	1369	1369	37	0	0	0	1369	1369	37	0	0	0	1369	1369	37
38	0	0	0	1444	1444	38	0	0	0	1444	1444	38	0	0	0	1444	1444	38	0	0	0	1444	1444	38
39	0	0	0	1521	1521	39	0	0	0	1521	1521	39	0	0	0	1521	1521	39	0	0	0	1521	1521	39
40	0	0	0	1600	1600	40	0	0	0	1600	1600	40	0	0	0	1600	1600	40	0	0	0	1600	1600	40
41	0	0	0	1681	1681	41	0	0	0	1681	1681	41	0	0	0	1681	1681	41	0	0	0	1681	1681	41
42	0	0	0	1764	1764	42	0	0	0	1764	1764	42	0	0	0	1764	1764	42	0	0	0	1764	1764	42
43	0	0	0	1849	1849	43	0	0	0	1849	1849	43	0	0	0	1849	1849	43	0	0	0	1849	1849	43
44	0	0	0	1936	1936	44	0	0	0	1936	1936	44	0	0	0	1936	1936	44	0	0	0	1936	1936	44
45	0	0	0	2025	2025	45	0	0	0	2025	2025	45	0	0	0	2025	2025	45	0	0	0	2025	2025	45
46	0	0	0	2116	2116	46	0	0	0	2116	2116	46	0	0	0	2116	2116	46	0	0	0	2116	2116	46
47	0	0	0	2209	2209	47	0	0	0	2209	2209	47	0	0	0	2209	2209	47	0	0	0	2209	2209	47
48	0	0	0	2304	2304	48	0	0	0	2304	2304	48	0	0	0	2304	2304	48	0	0	0	2304	2304	48
49	0	0	0	2401	2401	49	0	0	0	2401	2401	49	0	0	0	2401	2401	49	0	0	0	2401	2401	49
50	0	0	0	2500	2500	50	0	0	0	2500	2500	50	0	0	0	2500	2500	50	0	0	0	2500	2500	50
51	0	0	0	2601	2601	51	0	0	0	2601	2601	51	0	0	0	2601	2601	51	0	0	0	2601	2601	51
52	0	0	0	2704	2704	52	0	0	0	2704	2704	52	0	0	0	2704	2704	52	0	0	0	2704	2704	52
53	0	0	0	2809	2809	53	0	0	0	2809	2809	53	0	0	0	2809	2809	53	0	0	0	2809	2809	53
54	0	0	0	2916	2916	54	0	0	0	2916	2916	54	0	0	0	2916	2916	54	0	0	0	2916	2916	54
55	0	0	0	3025	3025	55	0	0	0	3025	3025	55	0	0	0	3025	3025	55	0	0	0	3025	3025	55
56	0	0	0	3136	3136	56	0	0	0	3136	3136	56	0	0	0	3136	3136	56	0	0	0	3136	3136	56
57	0	0	0	3249	3249	57	0	0	0	3249	3249	57	0	0	0	3249	3249	57	0	0	0	3249	3249	57
58	0	0	0	3364	3364	58	0	0	0	3364	3364	58	0	0	0	3364	3364	58	0	0	0	3364	3364	58
59	0	0	0	3481	3481	59	0	0	0	3481	3481	59	0	0	0	3481	3481	59	0	0	0	3481	3481	59
60	0	0	0	3600	3600	60	0	0	0	3600	3600	60	0	0	0	3600	3600	60	0	0	0	3600	3600	60
61	0	0	0	3721	3721	61	0	0	0	3721	3721	61	0	0	0	3721	3721	61	0	0	0	3721	3721	61
62	0	0	0	3844	3844	62	0	0	0	3844	3844	62	0	0	0	3844	3844	62	0	0	0	3844	3844	62
63	0	0	0	3969	3969	63	0	0	0	3969	3969	63	0	0	0	3969	3969	63	0	0	0	3969	3969	63
64	0	0	0	4096	4096	64	0	0	0	4096	4096	64	0	0	0	4096	4096	64	0	0	0	4096	4096	64
65	0	0	0	4225	4225	65	0	0	0	4225	4225	65	0	0	0	4225	4225	65	0	0	0	4225	4225	65
66	0	0	0	4356	4356	66	0	0	0	4356	4356	66	0	0	0	4356	4356	66	0	0	0	4356	4356	66
67	0	0</																						

Table 4 (cont.)

A large grid of numbers and labels, organized into columns and rows, representing data points for various categories like H=5 K=-5, H=6 K=2, etc.

Table 5. Planes in  $TATB$   $lX+mY+nZ+d=0$ 

	$l \times 10^2$	$m \times 10^2$	$n$	$d$	Angle with benzene ring ( $^\circ$ )
Benzene ring					
Spherical	-1.38	0.08	0.9999	-1.5365	—
Non-spherical	-1.37	0.15	0.9999	-1.5369	—
Nitro group I (C(1), N(1), O(1), O(2))					
Spherical	-5.12	-5.25	0.9973	-1.3738	3.75
Non-spherical	-5.01	-5.26	0.9974	-1.3780	3.67
Nitro group II (C(3), N(3), O(3), O(4))					
Spherical	3.30	-3.24	0.9989	-1.6411	3.33
Non-spherical	3.20	-3.14	0.9990	-1.6387	3.24
Nitro group III ((C(5), N(5), O(5), O(6)))					
Spherical	-3.60	1.46	0.9992	-1.4886	1.60
Non-spherical	-3.58	1.36	0.9993	-1.4868	1.40
Hydrogen Bond Group I (N(2), O(2), O(6'))					
Spherical	-4.20	-5.48	0.9976	-1.4281	3.57
Hydrogen Bond Group II (N(2), O(3), O(5'))					
Spherical	0.47	-1.74	0.9998	-1.5489	1.48
Hydrogen Bond Group III (N(4), O(4), O(2'))					
Spherical	2.01	-1.31	0.9997	-1.6072	2.10
Hydrogen Bond Group IV (N(4), O(5), O(1'))					
Spherical	7.88	6.60	0.9947	-1.6408	6.50
Hydrogen Bond Group V (N(6), O(6), O(4'))					
Spherical	-3.58	0.29	0.9994	-1.4450	1.28
Hydrogen Bond Group VI (N(6), O(1), O(3'))					
Spherical	-3.46	8.83	0.9955	-1.7012	5.17

No good basis could be established for choosing which of the different weighting schemes or atomic scattering factors gave the 'best' structure. However, because of the rarity of structure determinations in which non-spherical atomic scattering factors have been used, the results of this refinement and the corresponding refinement with spherical atomic scattering factors, both using unit weights, will be given. Results of calculations in which normal spherical atomic scattering factors were used will be identified as 'spherical', while results in which McWeeny's non-spherical atomic scattering factors were used will be identified as 'non-spherical'.

The final least-squares parameters for both refinements are given in Tables 2 and 3. In Table 4 are listed the final values, from the spherical refinement, of the calculated structure factors and the observed structure factors corrected for scale and extinction for which  $R=0.053$ . The corresponding tables for the non-spherical refinement and the different weighting schemes are available from the authors on request.

As a measure of the degree of completeness of the refinements, the average and maximum parameter shifts as fractions of the estimated standard deviations are 0.001 and 0.028, and 0.006 and 0.015 for the spherical and non-spherical refinements, respectively. The  $B$  parameter of H(1) is excluded in the spherical case because it was set equal to zero and not permitted to converge to a negative value. The fractional shift of this  $B$  parameter is 0.19.

#### Detailed description of the structure

Least-squares planes through the benzene ring, each of the nitro groups, and each of the six bifurcated hydrogen bonded groups were computed in an isometric-orthogonal system defined by the equations

Table 6. Distance from benzene plane

Atom	Spherical	Non-spherical
C(1)	0.02 Å	0.02 Å
C(2)	-0.02	-0.02
C(3)	-0.00	-0.00
C(4)	0.03	0.03
C(5)	-0.03	-0.03
C(6)	0.00	0.00
N(1)	0.09	0.08
N(2)	-0.09	-0.09
N(3)	0.00	-0.01
N(4)	0.09	0.09
N(5)	-0.08	-0.07
N(6)	-0.01	-0.01
O(1)	0.15	0.15
O(2)	0.04	0.04
O(3)	-0.07	-0.07
O(4)	0.05	0.05
O(5)	-0.09	-0.08
O(6)	-0.06	-0.06
H(1)	-0.13	-0.11
H(2)	0.01	0.05
H(3)	0.05	0.06
H(4)	0.08	0.07
H(5)	-0.03	-0.05
H(6)	-0.15	-0.18



Table 7. Distance from hydrogen bond planes  
(Spherical refinement)

Atom	Plane	Distance
H(1)	N(2), O(2), O(6')	-0.06 Å
H(2)	N(2), O(3), O(5')	+0.10
H(3)	N(4), O(4), O(2')	-0.04
H(4)	N(4), O(5), O(1')	+0.01
H(5)	N(6), O(6), O(4')	-0.01
H(6)	N(6), O(1), O(3')	-0.17

Table 8. Interatomic distances in TATB

Distance	Length (Å)	
	Spherical	Non-spherical
C(1)-C(2)	1.438	1.435 ± 0.007
C(2)-C(3)	1.443	1.448 ± 0.007
C(3)-C(4)	1.437	1.436 ± 0.007
C(4)-C(5)	1.447	1.446 ± 0.007
C(5)-C(6)	1.433	1.435 ± 0.007
C(6)-C(1)	1.446	1.450 ± 0.007
C(1)-N(1)	1.421	1.417 ± 0.007
C(2)-N(2)	1.312	1.310 ± 0.007
C(3)-N(3)	1.419	1.417 ± 0.007
C(4)-N(4)	1.322	1.320 ± 0.007
C(5)-N(5)	1.425	1.422 ± 0.006
C(6)-N(6)	1.314	1.311 ± 0.007
N(1)-O(1)	1.233	1.236 ± 0.006
N(1)-O(2)	1.243	1.243 ± 0.006
N(3)-O(3)	1.246	1.246 ± 0.006
N(3)-O(4)	1.241	1.239 ± 0.006
N(5)-O(5)	1.238	1.243 ± 0.006
N(5)-O(6)	1.254	1.253 ± 0.006
N(2)-H(1)	0.86	0.86 ± 0.07
N(2)-H(2)	0.89	0.85 ± 0.07
N(4)-H(3)	0.80	0.76 ± 0.07
N(4)-H(4)	1.05	1.06 ± 0.09
N(6)-H(5)	0.89	0.87 ± 0.08
N(6)-H(6)	1.06	0.96 ± 0.09
H(1)-O(2)	1.79	1.80 ± 0.07
H(1)-O(6')	2.41	2.40 ± 0.06
H(2)-O(3)	1.79	1.84 ± 0.07
H(2)-O(5')	2.36	2.37 ± 0.06
H(3)-O(4)	1.91	1.95 ± 0.07
H(3)-O(2')	2.37	2.39 ± 0.07
H(4)-O(5)	1.70	1.69 ± 0.08
H(4)-O(1')	2.24	2.24 ± 0.08
H(5)-O(6)	1.79	1.81 ± 0.08
H(5)-O(4')	2.37	2.37 ± 0.08
H(6)-O(1)	1.70	1.77 ± 0.09
H(6)-O(3')	2.24	2.35 ± 0.09

## Intramolecular hydrogen bonds

N(2)-O(2)	2.497	2.492 ± 0.007
N(2)-O(3)	2.482	2.484 ± 0.008
N(4)-O(4)	2.508	2.506 ± 0.007
N(4)-O(5)	2.478	2.480 ± 0.007
N(6)-O(6)	2.505	2.498 ± 0.007
N(6)-O(1)	2.486	2.492 ± 0.007

## Intermolecular hydrogen bonds

N(2)-O(5')	2.950	2.960 ± 0.006
N(2)-O(6')	2.995	2.995 ± 0.007
N(4)-O(1')	2.930	2.930 ± 0.006
N(4)-O(2')	2.989	2.989 ± 0.007
N(6)-O(3')	2.927	2.934 ± 0.006
N(6)-O(4')	2.991	2.993 ± 0.006

Table 9. Angles in TATB

Angle	Spherical	Non-spherical
C(6)-C(1)-C(2)	122.2	122.2 ± 0.4
C(6)-C(1)-N(1)	118.8	118.6 ± 0.4
C(2)-C(1)-N(1)	119.0	119.2 ± 0.5
C(1)-C(2)-C(3)	118.0	118.0 ± 0.5
C(1)-C(2)-N(2)	121.5	121.3 ± 0.5
C(3)-C(2)-N(2)	120.4	120.7 ± 0.5
C(2)-C(3)-C(4)	121.7	121.7 ± 0.4
C(2)-C(3)-N(3)	119.4	119.1 ± 0.4
C(4)-C(3)-N(3)	118.9	119.1 ± 0.4
C(3)-C(4)-C(5)	118.0	118.1 ± 0.4
C(3)-C(4)-N(4)	121.6	121.4 ± 0.5
C(5)-C(4)-N(4)	120.4	120.5 ± 0.5
C(4)-C(5)-C(6)	122.2	122.2 ± 0.4
C(4)-C(5)-N(5)	118.4	118.6 ± 0.4
C(6)-C(5)-N(5)	119.4	119.1 ± 0.4
C(5)-C(6)-C(1)	117.6	117.5 ± 0.4
C(5)-C(6)-N(6)	120.8	121.4 ± 0.5
C(1)-C(6)-N(6)	121.6	121.1 ± 0.5
C(1)-N(1)-O(1)	121.0	121.3 ± 0.4
C(1)-N(1)-O(2)	120.8	120.7 ± 0.4
O(1)-N(1)-O(2)	118.1	117.9 ± 0.4
C(3)-N(3)-O(3)	120.6	120.7 ± 0.4
C(3)-N(3)-O(4)	121.5	121.5 ± 0.4
O(3)-N(3)-O(4)	117.9	117.8 ± 0.4
C(5)-N(5)-O(5)	121.6	121.4 ± 0.4
C(5)-N(5)-O(6)	120.5	120.9 ± 0.4
O(5)-N(5)-O(6)	117.7	117.6 ± 0.4
C(2)-N(2)-H(1)	116	117 ± 4
C(2)-N(2)-H(2)	118	120 ± 4
H(1)-N(2)-H(2)	124	121 ± 6
C(4)-N(4)-H(3)	122	123 ± 6
C(4)-N(4)-H(4)	121	121 ± 4
H(3)-N(4)-H(4)	116	116 ± 7
C(6)-N(6)-H(5)	117	119 ± 5
C(6)-N(6)-H(6)	119	116 ± 5
H(5)-N(6)-H(6)	123	123 ± 7

## Non-bonded angles

H(1)-N(2)-O(2)	29	30 ± 4
H(1)-N(2)-O(6')	41	40 ± 4
H(2)-N(2)-O(3)	32	34 ± 4
H(2)-N(2)-O(5')	42	41 ± 4
H(3)-N(4)-O(4)	35	36 ± 6
H(3)-N(4)-O(2')	34	33 ± 6
H(4)-N(4)-O(5)	33	33 ± 4
H(4)-N(4)-O(1')	40	41 ± 4
H(5)-N(6)-O(6)	30	31 ± 5
H(5)-N(6)-O(4')	40	38 ± 5
H(6)-N(6)-O(1)	33	33 ± 5
H(6)-N(6)-O(3')	42	45 ± 5

$$X (\text{Å}) = ax + (b \cos \gamma)y + (c \cos \beta)z$$

$$Y (\text{Å}) = (b \sin \gamma)y - (c \sin \beta \cos \alpha^*)z$$

$$Z (\text{Å}) = (c \sin \beta \sin \alpha^*)z$$

as given by Chao & McCullough (1962). The equations for these planes are given in Table 5. The angles between the plane of the benzene ring and each of the other groups are also given in Table 5. Atoms labeled with primes are atoms of adjacent molecules (see Fig. 4). The distances of the atoms from the plane of the benzene ring are given in Table 6, and the distances of the hydrogen atoms from the planes of the three adjacent hydrogen bonded atoms are given in Table 7. The sign of the distance indicates the position of the atom above or below the plane. The

Table 10. *Magnitudes and direction angles, relative to the crystallographic axes, of the principal axes of the vibration ellipsoids*

Atom	Axis <i>i</i>	Spherical					Non-spherical				
		$B_i$ (Å <sup>2</sup> )	$a$ (°)	$b$ (°)	$c$ (°)	$c^*$ (°)	$B_i$ (Å <sup>2</sup> )	$a$ (°)	$b$ (°)	$c$ (°)	$c^*$ (°)
C(1)	1	1.1 ± 0.2	29 ± 23	92 ± 25	92 ± 12	79	0.7 ± 0.2	26 ± 65	95 ± 69	94 ± 28	83
	2	1.4 ± 0.2	116 ± 26	7 ± 13	115 ± 8	96	0.8 ± 0.2	114 ± 68	7 ± 54	114 ± 8	94
	3	3.0 ± 0.3	102 ± 6	83 ± 8	26 ± 7	12	3.3 ± 0.3	98 ± 5	85 ± 5	24 ± 5	8
C(2)	1	1.2 ± 0.2	12 ± 15	112 ± 16	86 ± 11	81	0.7 ± 0.2	3 ± 6	120 ± 18	89 ± 7	87
	2	1.6 ± 0.2	101 ± 17	27 ± 19	93 ± 22	71	1.2 ± 0.2	90 ± 18	32 ± 18	103 ± 7	80
	3	2.1 ± 0.3	96 ± 12	105 ± 20	4 ± 15	22	2.6 ± 0.3	93 ± 6	97 ± 7	13 ± 7	11
C(3)	1	1.8 ± 0.2	16 ± 16	135 ± 16	82 ± 15	86	1.0 ± 0.2	7 ± 22	113 ± 22	92 ± 9	87
	2	1.1 ± 0.1	75 ± 16	45 ± 16	106 ± 7	84	0.7 ± 0.2	97 ± 23	23 ± 23	109 ± 5	87
	3	2.5 ± 0.3	96 ± 14	91 ± 12	18 ± 9	8	3.1 ± 0.3	93 ± 6	92 ± 5	19 ± 4	4
C(4)	1	1.3 ± 0.2	37 ± 258	83 ± 263	110 ± 52	95	0.9 ± 0.2	26 ± 80	145 ± 82	87 ± 32	96
	2	1.3 ± 0.2	126 ± 261	9 ± 215	100 ± 91	84	0.8 ± 0.1	65 ± 82	55 ± 82	113 ± 6	91
	3	2.9 ± 0.3	82 ± 7	96 ± 6	23 ± 6	8	3.4 ± 0.3	84 ± 5	94 ± 4	23 ± 4	6
C(5)	1	1.4 ± 0.2	36 ± 31	84 ± 31	105 ± 14	90	0.6 ± 0.2	9 ± 207	111 ± 208	95 ± 85	90
	2	1.1 ± 0.2	126 ± 31	9 ± 25	113 ± 8	96	0.6 ± 0.2	99 ± 208	21 ± 207	114 ± 18	92
	3	3.7 ± 0.3	93 ± 5	84 ± 5	27 ± 5	6	4.2 ± 0.4	91 ± 4	88 ± 4	24 ± 3	2
C(6)	1	1.2 ± 0.2	18 ± 25	102 ± 25	97 ± 11	88	0.8 ± 0.2	11 ± 40	110 ± 42	93 ± 16	87
	2	1.5 ± 0.2	108 ± 25	12 ± 24	106 ± 11	85	1.0 ± 0.2	100 ± 42	20 ± 42	112 ± 6	90
	3	2.5 ± 0.3	91 ± 9	94 ± 11	18 ± 10	5	3.0 ± 0.3	93 ± 5	89 ± 6	22 ± 6	3
N(1)	1	1.6 ± 0.2	23 ± 31	143 ± 31	82 ± 13	89	1.3 ± 0.2	45 ± 54	165 ± 54	75 ± 19	89
	2	1.3 ± 0.1	67 ± 31	53 ± 31	113 ± 6	92	1.2 ± 0.1	45 ± 54	75 ± 54	109 ± 17	92
	3	4.3 ± 0.3	90 ± 4	88 ± 4	25 ± 3	2	3.9 ± 0.3	89 ± 4	89 ± 4	25 ± 4	2
N(2)	1	1.4 ± 0.2	38 ± 19	82 ± 19	109 ± 5	94	1.5 ± 0.2	22 ± 10	98 ± 11	105 ± 4	96
	2	1.0 ± 0.2	128 ± 19	8 ± 18	103 ± 6	87	0.8 ± 0.2	111 ± 10	9 ± 10	108 ± 4	88
	3	5.3 ± 0.3	85 ± 3	93 ± 2	24 ± 3	5	4.9 ± 0.3	83 ± 3	93 ± 2	24 ± 3	6
N(3)	1	1.9 ± 0.2	43 ± 9	162 ± 9	71 ± 5	84	1.6 ± 0.2	46 ± 12	165 ± 12	70 ± 5	85
	2	1.0 ± 0.1	47 ± 9	73 ± 9	105 ± 4	88	1.0 ± 0.1	45 ± 12	75 ± 12	105 ± 6	88
	3	4.6 ± 0.3	96 ± 3	86 ± 4	26 ± 4	6	4.2 ± 0.3	95 ± 4	85 ± 4	25 ± 4	6
N(4)	1	1.2 ± 0.2	6 ± 14	114 ± 14	94 ± 5	90	1.0 ± 0.2	5 ± 9	115 ± 9	92 ± 4	85
	2	1.8 ± 0.2	96 ± 14	24 ± 13	107 ± 4	85	1.8 ± 0.2	95 ± 10	26 ± 9	108 ± 4	86
	3	4.9 ± 0.3	90 ± 3	95 ± 3	18 ± 3	5	4.6 ± 0.4	91 ± 3	93 ± 4	18 ± 4	5
N(5)	1	1.8 ± 0.2	24 ± 21	96 ± 21	101 ± 10	90	1.5 ± 0.2	38 ± 31	82 ± 31	107 ± 12	92
	2	1.4 ± 0.2	114 ± 21	8 ± 15	115 ± 6	96	1.2 ± 0.2	128 ± 30	9 ± 28	110 ± 9	94
	3	3.5 ± 0.3	93 ± 5	84 ± 5	28 ± 5	6	3.2 ± 0.3	91 ± 5	86 ± 5	27 ± 5	4
N(6)	1	2.2 ± 0.2	18 ± 7	137 ± 7	90 ± 5	95	1.2 ± 0.2	22 ± 8	141 ± 8	89 ± 6	95
	2	0.9 ± 0.1	73 ± 7	47 ± 7	113 ± 2	91	0.8 ± 0.1	68 ± 8	52 ± 8	112 ± 3	90
	3	4.7 ± 0.3	85 ± 5	93 ± 4	23 ± 2	5	4.6 ± 0.4	85 ± 5	94 ± 4	22 ± 3	5
O(1)	1	1.3 ± 0.2	27 ± 10	93 ± 10	99 ± 4	87	1.2 ± 0.2	29 ± 8	91 ± 8	99 ± 3	86
	2	2.0 ± 0.2	117 ± 10	3 ± 10	109 ± 2	89	2.3 ± 0.2	119 ± 8	2 ± 7	108 ± 2	89
	3	10.1 ± 0.4	92 ± 1	90 ± 1	21 ± 1	3	9.5 ± 0.4	93 ± 2	91 ± 2	20 ± 2	4
O(2)	1	1.2 ± 0.2	16 ± 7	136 ± 7	85 ± 3	89	1.3 ± 0.2	18 ± 8	138 ± 8	84 ± 4	89
	2	2.3 ± 0.1	75 ± 7	46 ± 7	111 ± 2	89	2.5 ± 0.1	72 ± 8	48 ± 8	113 ± 3	91
	3	6.8 ± 0.3	92 ± 2	90 ± 2	22 ± 2	2	5.6 ± 0.3	91 ± 2	89 ± 3	24 ± 3	1
O(3)	1	2.2 ± 0.2	11 ± 12	131 ± 12	86 ± 4	89	2.6 ± 0.2	4 ± 8	134 ± 8	90 ± 3	90
	2	1.6 ± 0.2	79 ± 12	41 ± 12	110 ± 2	88	1.6 ± 0.2	86 ± 8	34 ± 8	111 ± 1	88
	3	10.9 ± 0.4	92 ± 1	91 ± 1	21 ± 1	3	10.3 ± 0.4	90 ± 2	91 ± 2	21 ± 1	2
O(4)	1	1.0 ± 0.1	32 ± 6	88 ± 6	105 ± 2	91	1.0 ± 0.1	33 ± 5	87 ± 5	107 ± 2	93
	2	2.3 ± 0.2	122 ± 6	2 ± 6	107 ± 3	89	2.6 ± 0.2	123 ± 5	4 ± 4	110 ± 3	93
	3	7.6 ± 0.3	88 ± 2	91 ± 2	23 ± 2	2	6.9 ± 0.3	89 ± 2	87 ± 3	27 ± 2	4
O(5)	1	1.3 ± 0.2	35 ± 7	154 ± 7	77 ± 3	88	1.3 ± 0.2	37 ± 7	156 ± 7	74 ± 3	85
	2	2.6 ± 0.1	56 ± 7	64 ± 7	106 ± 2	87	2.8 ± 0.1	54 ± 7	66 ± 7	108 ± 3	88
	3	8.2 ± 0.4	94 ± 2	90 ± 2	21 ± 2	4	7.5 ± 0.4	95 ± 2	86 ± 2	24 ± 2	5
O(6)	1	1.9 ± 0.2	17 ± 9	103 ± 9	95 ± 4	87	2.3 ± 0.2	10 ± 5	113 ± 7	88 ± 4	83
	2	1.2 ± 0.2	107 ± 9	13 ± 9	112 ± 2	91	1.3 ± 0.2	97 ± 7	23 ± 7	115 ± 2	93
	3	6.5 ± 0.3	94 ± 2	88 ± 2	23 ± 2	4	5.6 ± 0.3	98 ± 3	85 ± 3	25 ± 2	8

entire molecule is very nearly planar and lies almost exactly in the  $a$ - $b$  plane, making an angle of  $0.8^\circ$  with this plane.

Interatomic distances before correction for thermal motions are given for the spherical and non-spherical refinements in Table 8. The standard deviations are listed for the non-spherical case. These deviations were calculated using the entire variance-covariance matrix from the least-squares analysis, excluding unit cell parameter errors.

The intermolecular hydrogen bond distances as given in Table 8 are to molecules in the same layer. The closest inter-layer amino nitrogen-oxygen distance is  $3.36 \text{ \AA}$ . A similarly arranged list of bond angles is given in Table 9, and a diagram of the TATB molecule showing the uncorrected bond lengths is presented in Fig. 4.

The anisotropic thermal parameters were transformed to obtain the axes of the ellipsoids of thermal motion and the directions of these axes with respect to the crystallographic axes and  $c^*$ . These results are given in Table 10. As would be expected, the major axes of vibration for all atoms are nearly parallel to  $c^*$ . Another expected result is the observed increase in the amplitude of the thermal vibration of the carbon atoms perpendicular to the plane of the molecule on changing from spherical to non-spherical atomic scattering factors.

Translational and librational tensors were calculated (Cruickshank, 1956a) from the thermal parameters of the carbon and nitrogen atoms of the spherical refinement, using a code supplied by Trueblood (1962). The center of mass was taken as the unweighted average of the atomic positions. The oxygen atoms were omitted because examination of the ellipsoids of thermal vibration indicated a large torsional vibration of the nitro groups about the C-N bonds. The results of the calculation are given in Table 11.

Table 11. *Translational and librational tensors for the carbon and nitrogen atom skeleton*

Axes are the orthogonal set used in plane calculations

$$\tau = \begin{pmatrix} 0.0169 & -0.0009 & -0.0005 \\ & 0.0158 & -0.0003 \\ & & 0.0271 \end{pmatrix} \text{ \AA}^2$$

$$\sigma_\tau = \begin{pmatrix} 0.0013 & 0.0011 & 0.0014 \\ & 0.0013 & 0.0014 \\ & & 0.0022 \end{pmatrix} \text{ \AA}^2$$

$$\omega = \begin{pmatrix} 12.2 & -0.5 & -0.4 \\ & 12.9 & -0.1 \\ & & 2.1 \end{pmatrix} (\text{^\circ})^2$$

$$\sigma_\omega = \begin{pmatrix} 1.6 & 0.9 & 1.2 \\ & 1.6 & 1.2 \\ & & 0.9 \end{pmatrix} (\text{^\circ})^2$$

Corrections to the C-C and C-N distances were calculated by the method of Cruickshank (1956b, 1961). Corrections to the N-O distances were made assuming that the oxygen atoms vibrate in phase with the nitrogen atoms (Busing & Levy, 1964). This is a

minimum correction for the N-O distance. The average uncorrected and corrected bond distances are given in Table 12. An estimate of the torsional vibration of the nitro group about the C-N bond was made from the residual oxygen amplitudes perpendicular to the plane of the benzene ring and indicated an average amplitude of about  $12^\circ$ .

Table 12. *Average bond distances*  
(Spherical refinement)

Bond	Uncorrected	Corrected
C-C	1.441 \AA	1.444 \AA
C-N (nitro)	1.422	1.426
C-N (amino)	1.316	1.319
N-O	1.243	1.266

### Discussion of the structure

This compound contains a large number of unusual features. Some of these are the extremely long C-C bond in the benzene ring, the very short C-N (amino) bond, and the six bifurcated hydrogen bonds.

Bond order calculations were made (Pauling, 1960) using the corrected bond lengths from Table 12. These calculations indicate bond orders of 1.23 for the C-C, 1.02 for the C-N (nitro), 1.46 for the C-N (amino), and 1.52 for the N-O bonds. Summation over the entire molecule gives the anticipated total of six double bonds.

One can draw a large number of resonance forms for this molecule, some of which are given in Fig. 5.

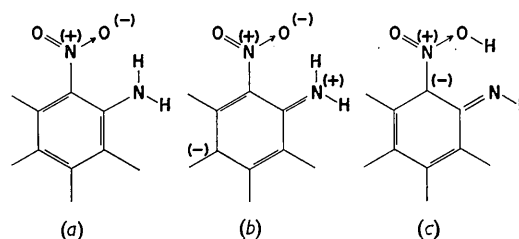


Fig. 5. Resonance forms of TATB.

The bond order calculations indicate that the normal resonance form [Fig. 5(a)] is relatively unimportant. Forms similar to Fig. 5(b) and (c) or with additional double bonds to other amino groups must contribute significantly to the structure. Resonance forms such as Fig. 5(c) and those in which the hydrogen bond has effectively withdrawn an electron from an adjacent molecule can be justified by an examination of the difference Fourier syntheses shown in Figs. 2 and 3, in which there are two regions of electron density, equal to or greater than  $\sigma_p$ , at about  $1 \text{ \AA}$  from each oxygen in reasonable locations. Evidence of a strong intermolecular interaction (hydrogen bond) in TATB is indicated by the lack of an observable melting point and low solubility in all solvents except concentrated sulfuric acid.

Another point which requires discussion is the systematic arrangement of peaks and valleys of residual electron density in the difference Fourier syntheses (Figs. 2 and 3). There are peaks of residual electron density approximately midway between the bonded carbon and nitrogen atoms, and valleys between the non-bonded carbon and nitrogen atoms of a molecule. These regions of residual electron density, both positive and negative, extend about 1 Å above and below the plane of the molecule. Integration of the residual electron density peaks, of the spherical refinement (Fig. 2), between the arbitrarily selected pairs of atoms C(3) and C(4), and C(5) and C(6) indicates that both of these regions contain approximately 0.1 electron in 1.3 Å<sup>3</sup>. Application of the methods suggested by McWeeny (1951, 1952, 1953, 1954) for X-ray scattering by bonded atoms would probably eliminate many of the systematic peaks and valleys of the difference Fourier synthesis. Application of these methods would account for some of the scattering power in the bonds and would reduce the apparent thermal motion in the plane of the molecule. This reduction in the apparent thermal motion would tend to remove electrons from the non-bonded regions and eliminate the valleys of the difference Fourier.

The authors wish to thank D. T. Cromer, R. B. Roof, and Prof. K. N. Trueblood for their interest

and discussions concerning this structure. Thanks are also due Mrs Lois Duncan for help in gathering the intensity data.

### References

- BUSING, W. R. & LEVY, H. A. (1964). *Acta Cryst.* **17**, 142.  
 CHAO, G. Y. & McCULLOUGH, J. D. (1962). *Acta Cryst.* **15**, 887.  
 CRUICKSHANK, D. W. J. (1949). *Acta Cryst.* **2**, 65.  
 CRUICKSHANK, D. W. J. (1956a). *Acta Cryst.* **9**, 754.  
 CRUICKSHANK, D. W. J. (1956b). *Acta Cryst.* **9**, 757.  
 CRUICKSHANK, D. W. J. (1961). *Acta Cryst.* **14**, 896.  
 EVANS, H. T., JR. (1961). *Acta Cryst.* **14**, 689.  
 FORSYTH, J. B. & WELLS, M. (1959). *Acta Cryst.* **12**, 412.  
 HOLDEN, J. R. (1962). Naval Ordnance Laboratory report NOLTR 62-46; [(1963). *C. A.* **59**, 13417h].  
 HOWELLS, E. R., PHILLIPS, D. C. & ROGERS, D. (1950). *Acta Cryst.* **3**, 210.  
 LIPSON, H. & COCHRAN, W. (1957). *The Determination of Crystal Structures*. 2nd ed., p. 300, London: Bell.  
 McWEENY, R. (1951). *Acta Cryst.* **4**, 513.  
 McWEENY, R. (1952). *Acta Cryst.* **5**, 463.  
 McWEENY, R. (1953). *Acta Cryst.* **6**, 631.  
 McWEENY, R. (1954). *Acta Cryst.* **7**, 180.  
 PAULING, L. (1960). *The Nature of the Chemical Bond*. 3rd ed., chap. 7. Ithaca: Cornell Univ. Press.  
 TRUEBLOOD, K. N. (1962). *I.U.Cr. World List of Crystallographic Computer Programs*. 1st ed., Groningen.  
 RAMACHANDRAN, G. N. & SRINIVASAN, R. (1959). *Acta Cryst.* **12**, 410.

*Acta Cryst.* (1965). **18**, 496

## The Crystal Structure of the Tetragonal Bronze Ba<sub>6</sub>Ti<sub>2</sub>Nb<sub>8</sub>O<sub>30</sub>

BY N. C. STEPHENSON

*School of Inorganic Chemistry, University of New South Wales, Sydney, Australia*

(Received 14 April 1964)

The structure of the tetragonal bronze Ba<sub>6</sub>Ti<sub>2</sub>Nb<sub>8</sub>O<sub>30</sub> has been determined by single-crystal X-ray analysis. The light-atom positions were determined from three-dimensional Fourier difference synthesis sections and the positional coordinates of all atoms were refined by cycles of differential syntheses. The Ti and Nb atoms are statistically distributed throughout the structure and are each surrounded by an octahedron of oxygen atoms. The metal-oxygen octahedra are joined together by corners in a framework containing four- and five-side tunnels which run through the structure. The barium ions fully occupy all available sites in these tunnels.

The space is *P4bm*. The metal atoms are displaced from the centres of gravity of the surrounding octahedra of oxygen atom. These displacements occur in the same direction resulting in a polar [001] axis, characteristic of a line ferroelectric.

### Introduction

The tetragonal tungsten bronze structure was deduced by Magnéli (1949) for the phase K<sub>x</sub>WO<sub>3</sub> (0.48 < x < 0.54). In this study, the positions of the tungsten and potassium atoms were found by single-

crystal techniques, but the oxygen atoms were placed in positions which afforded a reasonable stereochemical environment and were not confirmed by direct methods.

This structure arises not only in metal oxide 'bronzes' but in materials of high dielectric constant.